

# RESOURCE-EFFICIENT RGB-ONLY ACTION RECOGNITION FOR EDGE DEPLOYMENT

Dongsik Yoon\* Jongeun Kim\* Dayeon Lee\*

HDC LABS, Republic of Korea

## ABSTRACT

Action recognition on edge devices poses stringent constraints on latency, memory, storage, and power consumption. While auxiliary modalities such as skeleton and depth information can enhance recognition performance, they often require additional sensors or computationally expensive pose-estimation pipelines, limiting practicality for edge use. In this work, we propose a compact RGB-only network tailored for efficient on-device inference. Our approach builds upon an X3D-style backbone augmented with Temporal Shift, and further introduces selective temporal adaptation and parameter-free attention. Extensive experiments on the NTU RGB+D 60 and 120 benchmarks demonstrate a strong accuracy-efficiency balance. Moreover, deployment-level profiling on the Jetson Orin Nano verifies a smaller on-device footprint and practical resource utilization compared to existing RGB-based action recognition techniques.

**Index Terms**— Action Recognition, Efficient Video Understanding, Edge AI, TensorRT Deployment

## 1. INTRODUCTION

Human action recognition has long been a core challenge in video understanding, and remains central as deep learning continues to advance real-world perception capabilities [1, 2]. Accurate recognition of human actions is fundamental to many downstream applications, such as smart surveillance, human–robot interaction, assistive technologies, and context-aware analytics. In these settings, a system must capture not only the visual content of a scene but also the temporal structure of actions as they evolve over time.

As action recognition is increasingly used in real-world products and infrastructure, execution has shifted from datacenter scale GPUs to resource-constrained edge platforms such as embedded GPUs, on-device NPUs, and smart cameras. In many applications, edge-side inference is a necessity rather than a design choice, as it reduces latency, avoids reliance on unstable network connectivity, and mitigates privacy and bandwidth concerns by limiting raw video transmission. At the same time, moving action recognition models to edge devices introduces deployment-critical constraints that are often underrepresented in algorithm-centric evaluations.

In practice, low-power devices must operate under strict limits on throughput, memory, storage, and power or thermal budgets, frequently while sharing resources with other on-device workloads such as multi-camera decoding, detection and tracking, and system monitoring. These constraints give rise to several engineering challenges: model graphs that are difficult to optimize within embedded inference runtimes, large serialized engines that increase storage and update costs, elevated host and device memory usage that restrict workload concurrency, and sustained power draw that can trigger thermal throttling. As a result, application-aware evaluation must go beyond offline accuracy and consider metrics such as engine size, peak host memory, power consumption, and inference-time device memory usage.

Prior work has explored various directions to address these challenges. RGB-only action recognition has advanced through improved objectives and representation learning [3, 4, 5, 6, 7], while lightweight architectures have focused on efficient temporal modeling and mobile-friendly architectures [8, 9]. In parallel, many recent approaches improve accuracy–efficiency trade-offs by leveraging additional modalities, either at inference or as training-time guidance [9, 10, 11]. Although effective in benchmarks, reliance on auxiliary modalities at inference is often undesirable for real-world operation, as it requires external sensors or compute-intensive preprocessing (e.g., pose estimation) [12], increasing latency, resource usage, and system complexity.

In this work, we advocate treating **RGB-only inference as a first-class deployment target**, as it represents the lowest-assumption and most resource-efficient configuration for practical edge systems [13]. Motivated by this, we propose a compact RGB-only action recognition network explicitly designed for embedded execution. Our model builds on an efficient X3D-style backbone augmented with Temporal Shift for low-cost temporal modeling [14, 8], and further incorporates a parameter-efficient block structure inspired by mobile architectures, **selective temporal adaptation** applied only where it is most effective, and lightweight attention for feature refinement. We further ensure fair RGB-only comparisons by reconfiguring prior multi-modality models to the same inference setting [9]. Finally, beyond standard accuracy–efficiency metrics, we evaluate our approach under a unified embedded inference stack and report system-level on-device measurements, including engine size, peak RAM

\*Equal contribution.

usage, power consumption, and runtime device memory.

## 2. RELATED WORK

### 2.1. RGB-only Action Recognition

RGB-only action recognition has steadily advanced through improvements [3, 4, 5, 6, 7] in representation learning, objective design, and lightweight adaptation mechanisms—without relying on secondary modalities such as depth or skeleton. A notable trend is self-supervised pretraining for more transferable spatio-temporal features: ViewCLR [15] learns video representations via contrastive objectives while introducing additional feature-space transformations to improve generalization under distribution shifts. In supervised settings, contrastive formulations have also been used to better structure the embedding space; Shah et al. [16] leverages contrastive learning to enhance discriminability by forming semantically consistent positive pairs and enforcing separation from hard negatives. Going beyond objective design, DVANet [13] explicitly decomposes representation factors by disentangling action-relevant and nuisance components via a transformer-style decoding mechanism, improving recognition robustness under challenging capture conditions. More recently, large Vision-Language-Models have been explored as semantic priors for video understanding: VT-LVLM-AR [17] proposes a parameter-efficient adapter that maps long videos into compact temporal event representations and adapts a largely frozen LVLM via prompt tuning for fine-grained action recognition. Overall, many of these approaches remain difficult to run for real-time RGB-only action recognition, as they often introduce extra training/inference overhead—such as contrastive learning, disentanglement modules, or LVLM-based adapters—and fail to maintain favorable accuracy–efficiency trade-offs under tight latency and compute budgets.

### 2.2. Lightweight Action Recognition

Lightweight action recognition research primarily targets pragmatic limitations such as low latency, limited memory, and restricted compute budgets, which often make conventional 3D-CNN pipelines difficult to use. A representative approach replaces expensive 3D convolutions with 2D backbones augmented by inexpensive temporal mixing: EPAM-Net [9], for example, proposes X-ShiftNet, which integrates the Temporal Shift Module (TSM) [8] into an efficient 2D CNN to enable spatiotemporal modeling at substantially reduced computational cost, and further incorporates a pose-driven spatiotemporal attention block to highlight discriminative frames and regions while maintaining overall efficiency. Beyond architectural simplification, another emerging strategy exploits richer modalities only during training, while keeping inference lightweight. MMCL [10] follows this

principle by leveraging multi-modality co-learning with auxiliary instructive signals during training, then discarding the auxiliary pathways at test time to preserve single-modality inference. SV-data2vec [11] employs a student-teacher masked prediction scheme in which the teacher provides contextualized latent targets to guide the student representation learning, followed by downstream fine-tuning for action understanding.

Despite their efficiency-oriented designs, many of these methods still depend on additional modalities—such as skeleton or pose cues, or modality-specific teacher targets—to achieve their reported performance gains. Acquiring such secondary signals typically requires extra sensing or compute-intensive preprocessing (e.g., pose or skeleton estimation), which introduces non-negligible overhead and can become a practical bottleneck for strict real-time edge inference.

### 2.3. Efficient Architectural Primitives

Lightweight models increasingly benefit from reusable architectural primitives that improve accuracy–efficiency trade-offs with minimal overhead. Squeeze-and-Excitation Networks [18] introduces channel-wise feature recalibration via global pooling and lightweight gating, providing consistent gains with modest additional cost. GhostNet [19] reduces the heavy parameter/compute burden of pointwise convolutions by generating only a small set of intrinsic feature maps with standard convolution and synthesizing the rest using cheap operations. SimAM [20] further simplifies attention by deriving importance weights from an energy-based formulation, enabling parameter-free feature refinement without extra learnable modules. Most recently, MobileNetV4 [21] proposes the Universal Inverted Bottleneck as a flexible and hardware-aware building block and emphasizes Pareto-efficient designs across mobile targets. These primitives collectively motivate composing compact backbones by combining parameter-efficient blocks and lightweight attention mechanisms while keeping runtime overhead small.

## 3. METHOD

### 3.1. Overall Architecture

Our network is based on the X3D-style hierarchical design [14] combined with the Temporal Shift Module (TSM) [8] for low-cost temporal modeling. As illustrated in Fig. 1, the architecture consists of a stem layer, four stages, and a classification head. The stem applies a  $(1 \times 3 \times 3)$  convolution with stride  $(1 \times 2 \times 2)$  to reduce spatial resolution while preserving temporal information. Subsequent stages perform progressive spatial downsampling and channel expansion, followed by a  $1 \times 1 \times 1$  projection, global average pooling, and classification.

To balance efficiency and video action recognition performance, we integrate three complementary design choices:

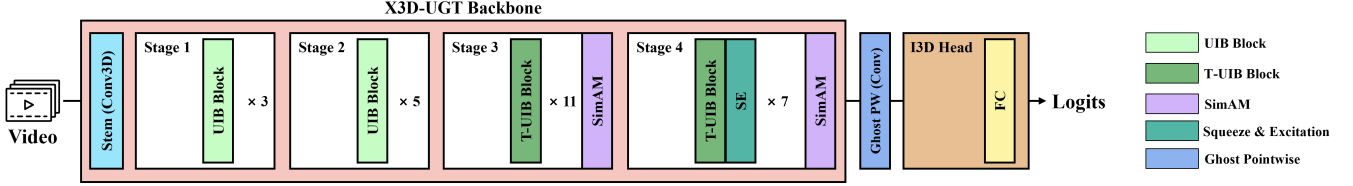


**Fig. 1.** Overview of the proposed RGB-only network (X3D-UGT) with UIB in Stages 1–2 and T-UIB in Stages 3–4.

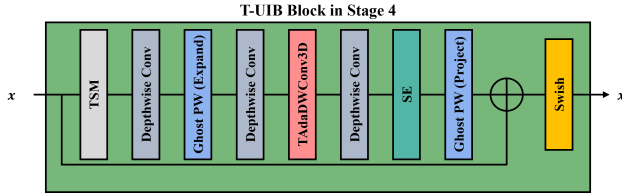


**Fig. 2.** Stage 4 T-UIB block: UIB with selective temporal adaptation (TAda) and lightweight pointwise design.

(1) a *parameter-efficient block structure* adapted from mobile architectures, (2) *selective temporal adaptation* applied only where it is most effective, and (3) *lightweight attention* for improved feature discrimination. The architecture is paired with a lightweight training objective that enhances convergence without increasing inference cost.

### 3.2. Efficient Building Blocks

#### Universal Inverted Bottleneck (UIB) for 3D features

The inverted bottleneck block follows an expand–depthwise–project pattern, where channels are first expanded, then processed by a depthwise operator, and finally projected back to a compact representation. We adapt the Universal Inverted Bottleneck (UIB) design from MobileNetV4 [21] to 3D video features by introducing an optional pre-depthwise spatial convolution that operates on the input channels prior to expansion. This pre-depthwise layer uses a  $(1 \times k \times k)$  kernel to refine spatial features at low cost, and performs spatial downsampling when required, allowing subsequent expanded features to be processed at reduced resolution.

For the mid-depthwise operation, we adopt the  $(2 + 1)$ D factorization strategy [22], decomposing depthwise 3D convolution into a  $(3 \times 1 \times 1)$  temporal convolution followed by a  $(1 \times k \times k)$  spatial convolution. This factorization explicitly separates temporal mixing from spatial processing, reducing computational cost while preserving receptive field coverage. As illustrated in Fig. 2, each block combines temporal shift for low-cost temporal mixing with the inverted bottleneck transformation, followed by projection and residual addition. Squeeze-and-excitation [18] is applied only in Stage 4 to maintain a favorable accuracy–efficiency balance.

#### Ghost pointwise convolution

Pointwise  $(1 \times 1 \times 1)$  convolutions dominate the parameter

count in inverted bottleneck architectures due to channel expansion. To mitigate this overhead, we extend the Ghost module [19] to 3D by replacing standard pointwise convolutions with a two-branch structure. A primary  $1 \times 1 \times 1$  convolution generates a subset of output channels, while the remaining channels are produced via a cheap depthwise convolution applied to the primary output. As shown in Fig. 2, this Ghost-based replacement is used for expansion and projection layers within each block, as well as for residual downsampling and the final feature projection layer.

### 3.3. Selective Temporal Adaptation and Training

#### Selective temporal adaptation

Temporal Adaptive Convolution (TAdaConv) [23] calibrates convolution responses based on temporal context, demonstrating strong performance in video understanding. However, applying temporal adaptation uniformly across all layers incurs noticeable computational overhead, as each adapted layer introduces additional gating whose complexity grows with channel width. We observe that temporal adaptation is not equally beneficial throughout the network: early layers primarily capture low-level spatial cues such as edges and textures that vary little across frames, whereas deeper layers encode semantic representations where temporal dynamics are more critical for distinguishing actions.

Motivated by this observation, we restrict temporal adaptation to a small number of blocks in the deeper stages. Specifically, TAda is enabled only in a subset of blocks in Stage3 and Stage4 (the first  $K$  blocks, with  $K = 2$  by default), as highlighted in Fig. 1. Following TAdaConv, rather than generating fully dynamic convolution kernels, we adopt a simplified variant that performs channel-wise residual scaling after a standard depthwise convolution. The gating signal is derived from temporally aggregated context using a lightweight bottleneck consisting of global spatial pooling followed by two  $1 \times 1$  convolutions with an intermediate depthwise temporal convolution. For stable optimization in training, the modulation is initialized as an identity mapping via a learnable blending coefficient initialized to zero, allowing the network to gradually incorporate temporal adaptation during training.

#### Parameter-free attention and training objective

To boost feature discrimination without adding learnable parameter count, we encompass SimAM [20] as a lightweight

Model	NTU 60		NTU 120		GFLOPs	Params (M)
	X-Sub	X-View	X-Sub	X-Set		
(Tran et al. 2015) (ICCV '15) [3]	63.5	70.3	-	-	38.5	78.4
(Baradel et al. 2018a) (CVPR '18) [4]	86.6	93.2	-	-	-	-
(Zhu et al. 2019) (SPL '19) [5]	93.2	97.7	-	-	51.7	33.0
(Vyas et al. 2020) (ECCV '20) [6]	88.9	86.3	-	-	-	-
(Cheng et al. 2022) [7]	91.9	95.4	-	-	-	-
ViewCLR (WACV '23) [15]	89.7	94.1	84.5	86.2	-	-
(Shah et al. 2023) (WACV '23) [16]	91.4	98.0	85.6	87.5	-	-
DVANet (AAAI '24) [13]	93.4	98.2	90.4	91.6	25.5	40.5
VT-LVLM-AR (Li et al. 2025) [17]	94.1	96.8	87.0	88.5	-	-
EPAM-Net (Neurocomputing '25) [9]	94.8	96.51	89.74	87.81	4.61	2.06
Ours	<b>95.21</b>	<b>98.31</b>	<b>90.88</b>	<b>92.67</b>	9.15	<b>0.96</b>

**Table 1.** Comparison with state-of-the-art **RGB-only** action recognition methods on NTU RGB+D 60 and NTU RGB+D 120. All results are reported using the **RGB modality only**. *Italic* values indicate results obtained by our re-implementation under the RGB-only setting, as the original EPAM-Net codebase is provided as an RGB+skeleton integrated framework.

Method	TAda Stage				Acc. (%) NTU60 X-Sub	Params (K)
	S1	S2	S3	S4		
v1	✓	✓	✓	✓	94.97	965
v2	✓	✓			95.08	930
v3		✓			95.06	934
v4			✓		94.87	955
Ours (w/o Poly-1)		✓	✓		95.10	962
Ours		✓	✓		<b>95.21</b>	962

**Table 2.** Ablation on stage-wise TAda placement.

attention mechanism. Since attention is most effective on high-level semantic features, we apply SimAM only after Stage 3 and Stage 4, adding negligible computational overhead due to its parameter-free element-wise formulation.

Finally, we train our network using Poly-1 loss [24], which augments standard cross-entropy with a polynomial term:

$$\mathcal{L}_{\text{Poly-1}} = \mathcal{L}_{\text{CE}}(p, y) + \epsilon \cdot (1 - p_y), \quad (1)$$

where  $\epsilon$  is a hyperparameter and  $p_y$  denotes the predicted probability for the ground-truth class. This loss strengthens gradients for misclassified samples, improving convergence while leaving inference unchanged.

## 4. EXPERIMENTS

### 4.1. Implementation Details

All experiments are implemented in PyTorch and trained with Distributed Data Parallel (DDP) on NTU RGB+D 60 and 120. Optimization is performed using SGD with an initial learning rate of 0.05, momentum 0.9, and weight decay  $3 \times 10^{-4}$ , scheduled by CosineAnnealingLR over 200 epochs. We adopt Poly-1 cross entropy loss with  $\epsilon = 1.0$ . Each input video clip is uniformly sampled to 16 frames and resized to  $224 \times 224$ .

During preprocessing, we apply a simple person-centric crop based on temporally smoothed 2D skeleton-derived bounding boxes with padding, and feed the resulting RGB clips to the network.

### 4.2. Comparisons to state-of-the-art

We investigate our approach with representative **RGB-only** action recognition methods on NTU RGB+D 60 and NTU RGB+D 120, as reported in Table 1. All models are evaluated using RGB inputs only, without depth or skeleton data. To ensure fair comparison, we re-train methods originally released as multi-modality pipelines under the RGB-only setting; in particular, EPAM-Net is re-trained without skeleton inputs, and the resulting accuracy is reported in Table 1.

Our method achieves strong performance across all evaluation protocols, reaching **95.21%** and **98.31%** on NTU 60 (X-Sub / X-View) and **90.88%** and **92.67%** on NTU 120 (X-Sub / X-Set), respectively. These results indicate that the proposed design maintains strong recognition accuracy while remaining lightweight and system-ready. Overall, the results support that our model achieves a favorable balance between accuracy and efficiency under the strict RGB-only constraints, aligning well with real-world embedded use scenarios.

### 4.3. Ablation Study

We investigate the impact of stage-wise TAda placement while keeping the training protocol fixed. As summarized in Table 2, placing TAda in deeper stages (S3, S4) is more effective than in early stages, supporting the intuition that temporal calibration works best on high-level semantic features. Notably, our final configuration (Ours) achieves the highest accuracy of 95.21% with only 962K parameters, demonstrating superior efficiency compared to the all-stage

Model	Modality	Params ↓	Acc* ↑	FPS ↑	Engine (MB) ↓	Peak RAM (MB) ↓	Power (W) ↓	TRT Ctx Mem (MiB) ↓
EPAM-Net [9]	RGB	2.06	96.5*	23.350	19.92	<b>3,141</b>	<b>12.824</b>	<b>80.2139</b>
DVANet [13]	RGB	40.5	98.2*	29.192	69.77	3,292	19.371	73.5
SVdata2vec [11]	RGB+S	18.4	99.3*	<b>51.259</b>	37.04	3,248	17.621	137.837
Ours	RGB	<b>0.96</b>	98.3*	10.305	<b>5.30</b>	3,153	16.947	89.8916

**Table 3.** Deployment-oriented profiling of various action recognition models on **Jetson Orin Nano** in MAXN SUPER mode using unified TensorRT FP16 inference. Here, S denotes the skeleton. **Acc\*** is *not* measured on the Jetson device; it is taken from the standard offline benchmark evaluation, while FPS, engine size, memory, and power are measured on-device.

version (v1). Furthermore, the inclusion of Poly-1 loss yields a 0.11% improvement over the version without it, confirming that our training objective effectively complements the selective temporal adaptation strategy.

#### 4.4. Edge Deployability Analysis

Table 3 presents a system-level comparison on Jetson Orin Nano in MAXN SUPER mode using a unified TensorRT FP16 inference pipeline. The reported **Acc\*** values are taken from offline NTU RGB+D evaluation on a server and are included for **reference only**; all runtime metrics—FPS, engine size, memory usage, and power consumption—are measured directly on the device. In addition to throughput, we report several metrics relevant to embedded execution to reflect the real-world restraints. Engine size (MB) indicates the serialized TensorRT plan file size, which affects storage requirements and OTA updates. Peak RAM (MB) captures the maximum host memory usage during inference, measured via `tegrastats`, and is critical when multiple services run concurrently. Power (W) indicates average device power draw, while TRT context device memory (MiB) measures GPU memory allocated for the TensorRT execution context, determining whether the model can coexist with other CUDA workloads.

Among the compared methods, our model achieves the smallest parameter count (0.96M) and the most compact engine size (5.30MB), which is approximately 3.7× smaller than EPAM-Net and 13× smaller than DVANet, substantially reducing the on-device storage requirements. Despite this compactness, it maintains strong recognition performance (98.3% Acc. in the offline benchmark), remaining competitive with heavier baselines such as DVANet (98.2%) while using only about 2.4% of its parameters. In terms of runtime behavior, our method exhibits peak RAM usage (3,153MB) comparable to other approaches and device power consumption (16.95W) within the range observed across baselines. Although its TensorRT context device-memory requirement (89.89MiB) is higher than EPAM-Net and DVANet, it remains substantially lower than SVdata2vec, indicating a manageable GPU-memory footprint. The main trade-off is inference throughput (10.3 FPS), which is lower than that of other methods but still suitable for many real-time scenarios. Overall, these results show that our approach provides the

most storage- and parameter-efficient solution while preserving competitive accuracy for resource-constrained embedded settings.

#### 4.5. Limitations

Although our model achieves the smallest parameter count (0.96 M) and the most compact TensorRT engine size (5.30 MB), its inference throughput on Jetson Orin Nano is constrained by TensorRT execution characteristics rather than model capacity. The architecture relies on multiple lightweight, memory-bound operators—including TSM-style temporal shift with tensor reshaping, Ghost pointwise convolutions, factorized UIB blocks, and TAda-based temporal calibration—which together produce a fragmented operator graph with many small CUDA kernels. On embedded GPUs, this leads to increased kernel-launch overhead and CPU-side scheduling cost, while providing limited arithmetic intensity to fully utilize Tensor Cores. Moreover, TensorRT is most effective when fusing large, compute-dense operators; the narrow channel widths and frequent depthwise and reshape operations in our design reduce fusion opportunities and shift performance bottlenecks toward memory bandwidth and dispatch latency. We estimate this limitation is primarily tied to the current embedded runtime and hardware configuration of our evaluation setup (Jetson Orin Nano with TensorRT), and is expected to be mitigated as edge accelerators and inference runtimes continue to mature.

## 5. CONCLUSION

We present a real-world-oriented RGB-only action recognition model that treats single-stream inference as a first-class target for edge systems. Built on an efficient X3D-style backbone with TSM, our method integrates a parameter-efficient block design (UIB + Ghost pointwise), selective temporal adaptation in deeper stages, and parameter-free attention to improve spatiotemporal discrimination under tight resource budgets. Experiments on NTU RGB+D 60/120 validate a strong accuracy–efficiency balance, and Jetson Orin Nano profiling under TensorRT FP16 confirms a compact engine footprint and practical resource usage, making the proposed approach suitable for real-world embedded systems.

## 6. REFERENCES

- [1] Yu Kong and Yun Fu, “Human action recognition and prediction: A survey,” *International Journal of Computer Vision*, vol. 130, no. 5, pp. 1366–1401, 2022.
- [2] Khaled Alomar, Halil Ibrahim Aysel, and Xiaohao Cai, “Cnns, rnns and transformers in human action recognition: a survey and a hybrid model,” *Artificial Intelligence Review*, vol. 58, no. 12, pp. 1–44, 2025.
- [3] Du Tran, Lubomir Bourdev, Rob Fergus, Lorenzo Torresani, and Manohar Paluri, “Learning spatiotemporal features with 3d convolutional networks,” in *Proc. ICCV*, 2015, pp. 4489–4497.
- [4] Fabien Baradel, Christian Wolf, Julien Mille, and Graham W Taylor, “Glimpse clouds: Human activity recognition from unstructured feature points,” in *Proc. CVPR*, 2018, pp. 469–478.
- [5] Jiagang Zhu, Wei Zou, Zheng Zhu, Liang Xu, and Guan Huang, “Action machine: Toward person-centric action recognition in videos,” *IEEE Signal Processing Letters*, vol. 26, no. 11, pp. 1633–1637, 2019.
- [6] Shruti Vyas, Yogesh S Rawat, and Mubarak Shah, “Multi-view action recognition using cross-view video prediction,” in *Proc. ECCV*, 2020, pp. 427–444.
- [7] Qin Cheng, Zhen Liu, Ziliang Ren, Jun Cheng, and Jianming Liu, “Spatial-temporal information aggregation and cross-modality interactive learning for rgb-d-based human action recognition,” *Ieee Access*, vol. 10, pp. 104190–104201, 2022.
- [8] Ji Lin, Chuang Gan, and Song Han, “Tsm: Temporal shift module for efficient video understanding,” in *Proc. ICCV*, 2019, pp. 7083–7093.
- [9] Ahmed Abdelkawy, Asem Ali, and Aly Farag, “Epamnet: An efficient pose-driven attention-guided multi-modal network for video action recognition,” *Neurocomputing*, vol. 633, pp. 129781, 2025.
- [10] Jinfu Liu, Chen Chen, and Mengyuan Liu, “Multi-modality co-learning for efficient skeleton-based action recognition,” in *Proc. ACM MM*, 2024, pp. 4909–4918.
- [11] Zorana Doždor, Tomislav Hrkać, and Zoran Kalafatić, “Sv-data2vec: Guiding video representation learning with latent skeleton targets,” in *Proc. WACV*. IEEE, 2025, pp. 6967–6976.
- [12] Min-Seok Kang, Dongoh Kang, and HanSaem Kim, “Efficient skeleton-based action recognition via joint-mapping strategies,” in *Proc. WACV*, 2023, pp. 3403–3412.
- [13] Nyle Siddiqui, Praveen Tirupattur, and Mubarak Shah, “Dvanet: Disentangling view and action features for multi-view action recognition,” in *Proc. AAAI*, 2024, vol. 38, pp. 4873–4881.
- [14] Christoph Feichtenhofer, “X3d: Expanding architectures for efficient video recognition,” in *Proc. CVPR*, 2020, pp. 203–213.
- [15] Srijan Das and Michael S Ryoo, “Viewclr: Learning self-supervised video representation for unseen viewpoints,” in *Proc. WACV*, 2023, pp. 5573–5583.
- [16] Ketul Shah, Anshul Shah, Chun Pong Lau, Celso M de Melo, and Rama Chellappa, “Multi-view action recognition using contrastive learning,” in *Proc. WACV*, 2023, pp. 3381–3391.
- [17] Kaining Li, Shuwei He, and Zihan Xu, “VT-LVLM-AR: A video-temporal large vision-language model adapter for fine-grained action recognition in long-term videos,” *arXiv preprint arXiv:2508.15903*, 2025.
- [18] Jie Hu, Li Shen, and Gang Sun, “Squeeze-and-excitation networks,” in *Proc. CVPR*, 2018, pp. 7132–7141.
- [19] Kai Han, Yunhe Wang, Qi Tian, Jianyuan Guo, Chunjing Xu, and Chang Xu, “Ghostnet: More features from cheap operations,” in *Proc. CVPR*, 2020, pp. 1580–1589.
- [20] Lingxiao Yang, Ru-Yuan Zhang, Lida Li, and Xiaohua Xie, “SimAM: A simple, parameter-free attention module for convolutional neural networks,” in *Proc. ICML*, 2021, pp. 11863–11874.
- [21] Danfeng Qin, Chas Leichner, Manolis Delakis, Marco Fornoni, Shixin Luo, Fan Yang, Weijun Wang, Colby Banbury, Chengxi Ye, Berkin Akin, et al., “MobileNetV4: Universal models for the mobile ecosystem,” in *Proc. ECCV*, 2024.
- [22] Du Tran, Heng Wang, Lorenzo Torresani, Jamie Ray, Yann LeCun, and Manohar Paluri, “A closer look at spatiotemporal convolutions for action recognition,” in *Proc. CVPR*, 2018, pp. 6450–6459.
- [23] Ziyuan Huang, Shiwei Zhang, Liang Pan, Zhiwu Qing, Mingqian Tang, Ziwei Liu, and Marcelo H Ang Jr, “TAda! temporally-adaptive convolutions for video understanding,” in *Proc. ICLR*, 2022.
- [24] Zhaoqi Leng et al., “PolyLoss: A polynomial expansion perspective of classification loss functions,” in *Proc. ICLR*, 2022.